This is an open access article published under a Creative Commons Attribution (CC-BY) License, which permits unrestricted use, distribution and reproduction in any medium, provided the author and source are cited.

ACS AUTHORCHOICE

ACS APPLIED MATERIALS & INTERFACES

www.acsami.org

Research Article

Inkjet Printable Polydimethylsiloxane for All-Inkjet-Printed Multilayered Soft Electrical Applications

Riikka Mikkonen,* Paula Puistola, Ilari Jönkkäri, and Matti Mäntysalo

Cite This: *ACS Appl. Mater. Interfaces* 2020, 12, 11990–11997

Read Online

ACCESS | Metrics & More | Article Recommendations | Supporting Information

ABSTRACT: In recent years, additive manufacturing of polydimethylsiloxane (PDMS) has gained interest for the development of soft electronics. To build complex electrical devices, fabrication of multilayered structures is required. We propose here a straightforward digital printing fabrication process of silicone rubber-based, multilayered electronics. An inkjet-printable PDMS solution was developed for the digital patterning of elastomeric structures. The silicone ink was used together with a highly conductive silver nanoparticle (Ag NP) ink for the fabrication of all-inkjet-printed multilayered electrical devices. The application of the multilayered circuit board was successful. The sheet resistances were below 0.3 Ω/□, and the conductive layer thickness was less than 1 μm. The electrical insulation between the conductive layers was done by printing a 20−25 μm-thick dielectric PDMS layer selectively on top of the bottommost conductive layer.

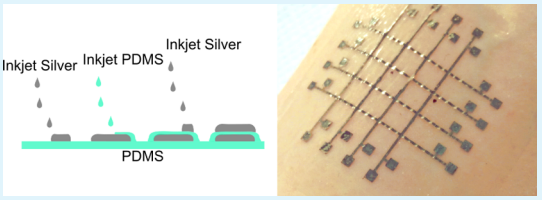

KEYWORDS: *polydimethylsiloxane, elastomer, dielectric, inkjet printing, multilayer, printed electronics*

Downloaded via TAMPERE UNIV on April 15, 2020 at 09:06:28 (UTC).
See https://pubs.acs.org/sharingguidelines for options on how to legitimately share published articles.

INTRODUCTION

Polydimethylsiloxane (PDMS) is a widely used silicone elastomer because of its biocompatibility, low cost, and optical transparency. Properties such as nontoxicity, chemical inertness, and high elasticity make it suitable for both in vitro and in vivo applications, including, for example, tissue mimicking, electronic skin (e-skin) applications, and microfluidics.[1−4]

In order to fabricate 3D-shaped PDMS structures conventionally by means of lithography or mold casting, several process steps and tools, such as mask aligners, evaporation or sputter deposition tools, and etching equipment, are required. In addition, the fabrication process may require using hazardous chemicals.[5,6] To address the inconvenience of these PDMS fabrication processes, several approaches of additive manufacturing have been presented in recent years, including 3D printing of PDMS using supportive baths and gels,[7,8] and curing with either heat or UV light.[9−11] Additive manufacturing enables more rapid prototyping and iteration rounds at a low cost, and even complex shapes imitating human hands or blood vessels can be fabricated.[10]

Digital drop-on-demand (DOD) printing is a great example of additive manufacturing techniques. These digital printing techniques, such as inkjet printing, can be used both in laboratory prototyping and on an industrial scale.[12,13] The main benefits of these techniques include low material consumption and contactless printing. Sturgess et al. presented an approach[14] where PDMS was DOD inkjet-printed to produce ziggurat-shaped 3D objects. They used the two components of Sylgard 184 silicone as inks, and these components were printed sequentially. Thus, the elastomer was cross-linked in the process.

In addition to the abovementioned benefits, the inkjet printing technology is also compatible with large or irregularly shaped substrate materials. Therefore, DOD printing is a promising technology for the manufacturing of soft, large area, flexible, and stretchable electronics. Examples of inkjet-printed, wearable devices include tattoo-like devices,[15] piezoelectric devices,[16,17] and other skin-conformable systems.[18,19] To apply the inkjet printing of PDMS in electronic fabrication, McCoul 3D inkjet-printed commercial silicone elastomer foils were used for dielectric elastomer actuators.[20] In the approach of Peng et al., an inkjet printable PDMS was used to make microlens arrays for pressure sensors.[21] In order to fabricate printed functional systems from passive components to the final devices, deposition of more than one material is required.[22−27] Mamidanna et al.[28] fabricated a PDMS-based microfluidic mixer by inkjet printing, including the fluid channels and sensing electrodes.

This work presents a straightforward fabrication strategy for multilayered, all-inkjet-printed soft electrical systems in an elastomeric matrix. In contrast to the previous approaches,[14,20] we printed the whole functional structure, including the conductive material and the dielectric material, with a single material printer. The key component of this approach is our PDMS (Sylgard 184) ink, which is used as a dielectric between

Received: October 30, 2019
Accepted: February 13, 2020
Published: February 13, 2020

© 2020 American Chemical Society

https://dx.doi.org/10.1021/acsami.9b19632
ACS Appl. Mater. Interfaces 2020, 12, 11990−11997

the conductive tracks. The work herein includes the characterization of silicone ink properties, such as viscosity and surface tension measurements, and printing trials for optimization of jetting stability and patterning of the dielectric ink. The ink was tuned to be compatible with the Fujifilm Dimatix DMP inkjet printers, which are widely used to print patterns for printed electronic applications.[29−33]

Printing of our PDMS ink was allowed at 30 °C temperature for at least 2 days with one cartridge, when stored in a refrigerator overnight, even though the polymer was mixed in advance. This is a significant improvement to the previous work, where the ink with a premixed PDMS component was reported to remain printable for only 2 h.[28] Even though the reactive printing strategy, where the two PDMS components are printed separately and mixed in situ, would allow an even longer shelf-life for the inks, using more than one ink cartridge to print one material will add steps to the fabrication process and make it both slower and less convenient.

Together with a highly conductive Ag NP ink, the optimized dielectric ink was used to print conductive lattice structures as a demonstration of an all-inkjet-printed, multilayered system. The results indicate that the printing of the elastomeric dielectric layers enables the additive and digital manufacturing of complex electrical devices. This is a great benefit in comparison to the processes, which are based on a PDMS casting process, where the fabrication of multilayered electronics will require using stencils, via structures and punching tools.[34,35] With sufficient patterning geometry and material selection, this process is easily applicable to the manufacturing of soft, biocompatible, and skin-conformable electrical devices entirely by inkjet printing, with only a few process steps.

RESULTS AND DISCUSSION

Herein, two ink solvents were used. Isobutyl acetate (IBA) was selected as a less hazardous substitute for toluene used by Mamidanna et al.[28] Peng et al.[21] used *n*-butyl acetate successfully with a 50 μm nozzle diameter in a Microfab jetlab II-printer. Here, the performance of the solvent was studied using a Dimatix DMP 2800-printer with a 21 μm nozzle diameter. Octyl acetate (OA) was selected as a slower-evaporating, nonhazardous alternative. It has been previously found to be a promising PDMS solvent by Sturgess et al.[14] The mixed Sylgard 184 (1:10) was diluted in both OA and IBA. The objective was to produce a well-working ink for the DMP-2800 inkjet printer, and therefore, the target viscosity was set to 10−20 mPa·s and the target surface tension to 20−35 mN/m.

First, the viscosities of different silicone inks were measured as a function of the shear rate from 1 to 1000 1/s (Figure 1a) to estimate inks' jettability at the printing frequency. The shear rate of the liquid in the nozzle is dependent on the piezoelectric actuator's motion and may reach values up to 40 kHz.[36] Therefore, the ink viscosity's response to higher shear rates is crucial to understand, when the ink jettability is estimated. Ink viscosities were also measured as a function of increasing temperature from 25 to 70 °C (Figure 1b). Even though the cartridge temperature is set to a low value, information on the viscosity at elevated temperatures is beneficial. When the height distance between the nozzles and the substrate is only 0.8 mm, heating of the substrate (60 °C) will also elevate the cartridge temperature (approx. 5 °C)

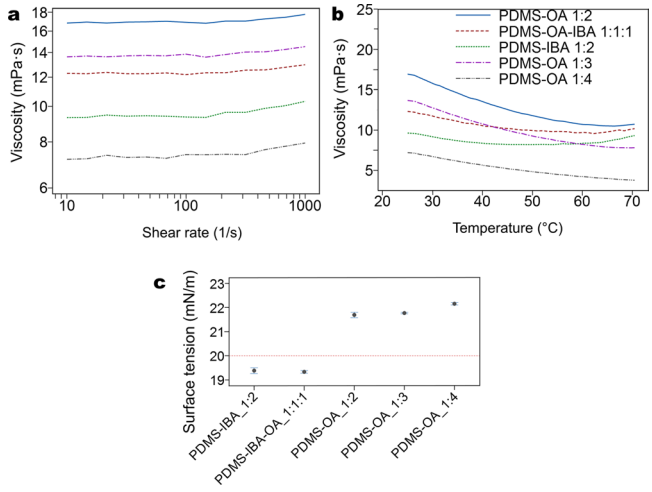

Figure 1. Summary of the fluid characteristics of all the ink solutions; the data labels are the same for both (a,b). (a) Measured viscosities of different ink compositions as a function of the shear rate (1−1000 1/s). One measurement per ink is given. (b) Measured viscosities as a function of the temperature (25−70 °C). One measurement per ink is given. (c) Measured surface tensions (15 measurements, confidence interval CI 95% for the mean).

during printing because there is no cooling element in the cartridge.

All viscosities remained rather stable during the shear rate tests, indicating Newtonian behavior. Some differences were observed in the temperature tests: the viscosities of all inks decrease with increasing temperature; a deeper slope is observed with the OA-diluted inks, whereas the IBA solvent leads to a moderate decrease in the viscosity. Additionally, a moderation of the slope can be observed at the higher end of the temperature range (50−70 °C), and even an increment of the viscosity is observed. The significant viscosity slope moderation of the IBA-containing solutions and their clear viscosity increment at higher temperatures are suspected to be an outcome of the accelerated solvent evaporation of this relatively volatile solvent (vapor pressure 20 hPa at 20 °C and low boiling point 120 °C), resulting in a higher PDMS concentration, when the solution is heated. With lower polymer concentrations (20−25% by weight), the moderation of the viscosity slope is less significant at elevated temperatures or is not observed at all.

In addition to the viscosity measurements, the surface tensions of the ink solutions were measured (Figure 1c). We observed that only the surface tensions of the OA-based inks were in the theoretical printable range (γ > 20 mN/m) and that the ink surface tension increased with higher OA-content.

The results of viscosity and surface tension measurements were clearly observed in the ink-jetting trials: Either of the IBA-containing inks could not be jetted successfully, which is most likely due to both the inadequate surface tension and the relatively high evaporation rate of the solvent, in comparison to the OA-diluted solutions. Droplets could be jetted for a short time, but the nozzles were clogging too quickly, preventing a reliable and reproducible jetting. Interestingly, the *Z*-numbers, which are commonly used to evaluate the printability of the inkjet inks,[20,37] were all in the range of $1 < Z < 3$ for our inks (Table S1).

However, it has been argued in the literature that there are many other parameters affecting the final jetting behavior and

https://dx.doi.org/10.1021/acsami.9b19632
ACS Appl. Mater. Interfaces 2020, 12, 11990−11997

printability, especially in the case of polymer inks. These parameters include, for example, the solvent vapor pressure, the molecular weight, and the concentration of the polymer.[38−40] Nevertheless, Peng et al. used *n*-butyl acetate successfully to dilute PDMS for inkjet printing in a 1:3 ratio (PDMS to solvent).[21] To investigate IBA jetting further, we prepared a 1:3 PDMS−IBA solution for jetting trials. The droplet firing was better than that with the 1:2 solution, but the nozzles still clogged very quickly. Only a frequent cleaning cycle could keep the nozzles firing, but even then, the droplets were heavily misdirected. Therefore, this ink was declared to be not stable enough for printing. A 1:4 solution was not prepared because the measurement results (Figure 1a−c) indicate that the viscosity will decrease far below 10 mPa·s, and the surface tension of the ink will not increase significantly with a higher solvent concentration, meaning no improvement in the ink's properties. The main difference between our approach and that of Peng et al. is the ink volume in the printhead: our nozzle diameter is only 21 μm, whereas their nozzle diameter was 50 μm.[21] Therefore, the ink volume in our printhead is significantly smaller, and the ink is likely to be more sensitive to the effects of surface tension, viscosity, or solvent vapor pressure.

The jetting of the octyl acetate-based inks was found to be sufficient for further trials. However, because the two components of Sylgard 184 were mixed in advance to the printing, it was necessary to keep the cartridge temperature as low as possible, thus hindering the cross-linking of the PDMS component. The 1:2 PDMS−OA solution required heating the cartridge to temperatures above 35 °C, and therefore it was discarded before further experiments. Both the 1:3 and 1:4 PDMS−OA solutions could be printed without heating the cartridge above 30 °C. To maximize the PDMS-content of the ink, we chose to use the 1:3 PDMS−OA solution instead of the 1:4 PDMS−OA solution. This solution remained printable for at least 2 days without the need to modify the cartridge settings, when the ink cartridge was stored in the refrigerator overnight.

The contact angles of the 1:3 PDMS−OA solution were measured on the spin-coated PDMS and on the printed silver surface to estimate its printability as a dielectric layer. The ink contact angles were 46 ± 1 and ≤15°, respectively. In the printing trials, it was observed that the droplet size on the substrate, which is equal to one pixel of a raster image, was approximately 45 μm, and that the well-defined, continuous lines could be printed on the PDMS substrate using a drop spacing (DS) of 20 μm. In Figure 2a, the measured line widths are presented for 2-pixel (2px), 4-pixel (4px), and 6-pixel (6px) lines from top to bottom, respectively.

The Raman data on the prints against the spectra of the cast reference PDMS and octyl acetate are shown in Figure 2b. In both the printed and cast reference PDMS spectra, strong characteristic peaks can be seen at 2904 and 2965 cm^{-1}, indicating CH_3 stretching.[41] Other strong PDMS peaks can be seen at 1410 and 1264 cm^{-1}, indicating asymmetric and symmetric CH_3 bending.[41] A PDMS peak at 862 cm^{-1} corresponds to symmetric CH_3 rocking, whereas a peak at 786 cm^{-1} indicates asymmetric CH_3 rocking and asymmetric Si−C stretching. Another characteristic peak of PDMS can be found at 710 cm^{-1}, corresponding to Si−C symmetric stretching. Finally, a peak at 490 cm^{-1} indicates the symmetric stretching of Si−O−Si. These peaks are visible in the spectra of both the ink-jetted PDMS and the reference PDMS. The

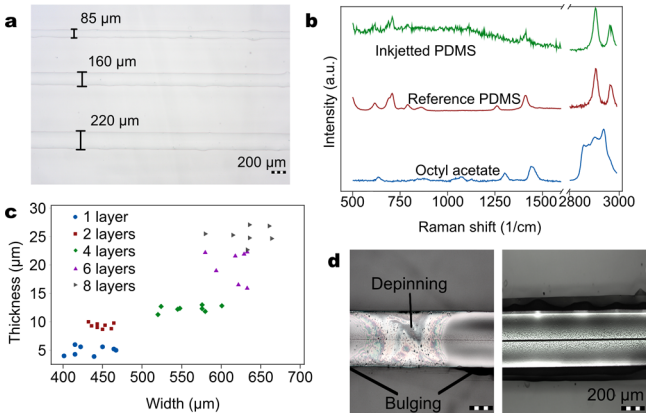

Figure 2. Properties of the printed PDMS. (a) Lines (width: 2 pixels (px), 4 pixels (px), and 6 pixels (px)) on a PDMS substrate, DS 20 μm. (b) Raman spectra of the printed sample (8 layers, DS 20 μm, 120 °C/20 min) against the cast reference PDMS and octyl acetate. (c) Thickness as a function of the pattern width, one to eight layer square patterns printed on the spin-coated PDMS. (d) Left: dielectric ink depinning from the silver surface, direct printing, right: dielectric ink covering the bottom trace, an improved printing strategy.

strong peaks in the octyl acetate spectrum can be found at 2859−2941 cm^{-1}, where a wide peak is shown. Additional peaks are at 637, 660, 1129, 1307, and 1743 cm^{-1}. Even though the background signal adds some noise to the spectrum of the thin printed PDMS sample, none of these octyl acetate's characteristic peaks are clearly visible. Therefore, it can be concluded that the final printed and cured PDMS is free of solvent residues and resembles the cast PDMS. Thus, similar curing conditions as in the traditional casting process can be used.

Printing with the 1:3 PDMS−OA solution led to an approximately 5 μm dry layer thickness, and printing with eight passes led to a 25 μm thickness, when printed on the PDMS substrate (Figure 2c). Ink spreading is well controlled on a hydrophobic PDMS substrate, and when small enough volumes of ink are added on top of the existing layers (Figure 2c: 1 layer and 2 layers), the pattern will not spread and the thickness can be built effectively. When the volume of the wet ink is high enough, the pattern will spread and only a moderate increment in thickness is observed, as shown in Figure 2c with four layers. When more layers are printed, the thickness is again built effectively, but the pattern does not spread significantly (Figure 2c, six layers and eight layers).

On the other hand, printing the PDMS ink on silver was prevented as such due to ink depinning and uncontrolled coalescence (Figure 2d). To control the ink coalescence on the silver surface, the PDMS ink was first printed next to the silver track to form borderlines and to act as contact points. After drying the ink, we filled the enclosed silver surface with the PDMS ink (Figure 2e). Printing five to eight layers of the PDMS resulted in uniform lines, insulating the underlying silver. To ensure the best possible electrical insulation between the conductive tracks, eight-layer PDMS prints were used in further printing trials.

To demonstrate the functionality of the developed PDMS ink, we fabricated a silicone elastomer-based two-layered conductive lattice structure with an electrically insulating PDMS layer. The hydrophobicity of the PDMS surface prevented printing of the Ag NP ink on top of the native PDMS substrate as such. As reported in the literature, it is

https://dx.doi.org/10.1021/acsami.9b19632
ACS Appl. Mater. Interfaces 2020, 12, 11990−11997

necessary to treat the hydrophobic PDMS surface at least with plasma or UV-ozone before coatings can be applied.[42−46] We chose nitrogen plasma for the pretreatment for conductive track printing. Previously, it has been found to enable slower hydrophobic recovery of the treated PDMS in comparison to the oxygen plasma treatment.[46,47] Here, the nitrogen plasma treatment also provided better wetting of the Ag NP ink on the PDMS substrate in comparison to the oxygen plasma. Because the printed PDMS's hydrophobicity was observed to be similar to that of the cast PDMS, an additional plasma treatment was applied to the structure after printing the dielectric layer.

In addition to the ink-wetting challenges, the interface behavior between the PDMS layers and the silver tracks at elevated temperatures proved to be another challenge. The silver tracks tended to wrinkle and crack (Figure 3a−c). This

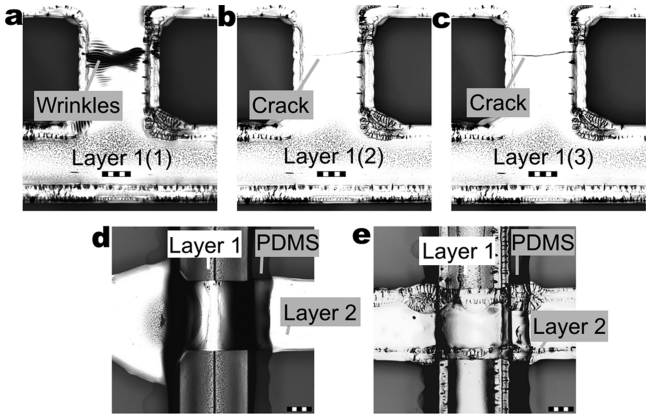

Figure 3. (a) Wrinkling of the bottommost silver track after curing [Layer1 (1)]. (b) Cracking of the wrinkled area after the dielectric printing and curing [Layer 1(2)]. (c) Crack propagation of the previous area after the topmost silver track printing and curing [Layer 1(3)]. (d) Ink flooding into the intersection of the conductive tracks, one printing pass. (e) Well-defined intersection of the conductive tracks, improved patterning strategy. Scale bar 200 μm.

behavior is most likely caused by the mismatch of the material coefficients of thermal expansion (CTE) and the Ag NP densification upon curing.[48−51] Another challenge was the flooding of the Ag NP ink at the intersection of the silver tracks, when the topmost track was printed in one pass (Figure 3d).

The optimized curing conditions for the Ag NP ink (120 °C/30 min) together with an improved printing strategy enabled the fabrication of pristine conductive lines (Figure 3e). We used here a similar patterning strategy as with the PDMS layer: first, we printed the outlines of the conductive tracks, let the print dry and settle, and followed it with pattern filling. This strategy also enabled the printing of well-defined tracks on top of the 3D surface formed by the insulated silver track (Figure 3e).

Once both the surface treatment parameters and printing strategy were optimized, we fabricated the final multilayered lattice structures (Figure 4a,b). The cross-sectional images of the topmost trace (Figure 4d), the intersection of the conductive tracks (Figure 4e−g), and the encapsulated bottommost trace (Figure 4h) show that the thickness of the printed dielectric on the silver surface is approximately 20−25 μm in the middle of the dielectric layer. The cross-sectional images revealed that the thickness of the dielectric was the highest in the center of the line, and was found to decrease

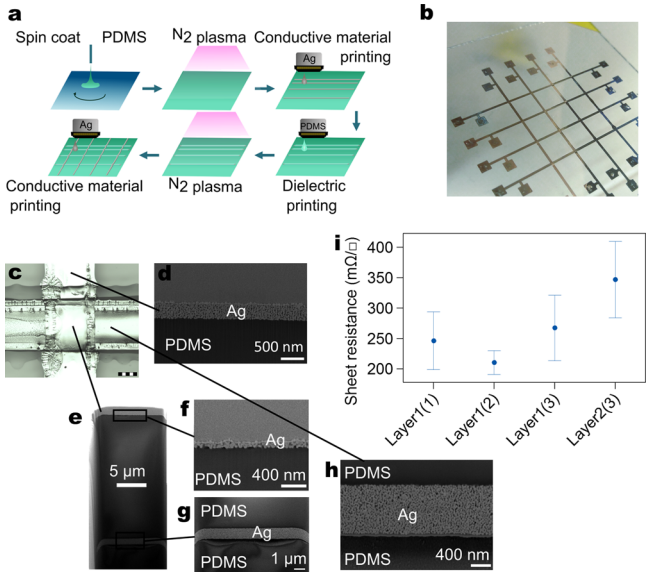

Figure 4. (a) Schematics of the fabrication process. (b) Photograph of the fabricated multilayered structure. (c) Microscopy image of a track intersection. Scale bar 200 μm. (d) Cross-sectional image of the topmost silver layer. (e) Cross-sectional image of the track intersection. (f) Cross-sectional image of the topmost silver layer at the intersection. (g) Cross-sectional image of the bottommost silver layer at the intersection. (h) Cross-sectional image of the bottommost silver layer. (i) Measured sheet resistances of the bottommost silver tracks after silver ink curing [Layer 1(1)], after dielectric curing [Layer 1(2)], and after topmost silver ink curing [Layer 1(3)] and the sheet resistances of the topmost silver tracks after curing [Layer 2(3)]. 24 measurements, confidence interval for the mean is 95 %.

toward the side, where the dielectric thickness was only approximately 10 μm, leading to a dome-like profile. The thickness of the conductive tracks was 500 nm^{-1} μm at the bottom conductor layer (Figure 4e−h) and 100−500 nm at the top conductor layer (Figure 4d−f). A partial delamination of the bottom silver layer from the substrate was observed in some cross-sectional images (Figure 4g,h). This is suspected to be a combination of the stresses from the cross-section sample fabricated by focused ion beam (FIB) and adhesion issues of the Ag NP−PDMS interface, making it more vulnerable to the stresses caused by the FIB process.

On the other hand, the printed PDMS layer seems to adhere better to the porous Ag NP structure above (Figure 4g,h). This finding is in line with previous literature reports, which suggest that casting the liquid PDMS over conductive Ag structures (NPs, flakes, nanowires, etc.) with a consequent curing step can provide better adherence of the metal layer to the elastomer in comparison to the metal coating of the hard-cured PDMS.[34,35,52−54]

In the resistance measurements, the inevitable degrading effect of the CTE mismatch during the repeated heat-curing steps was observed (Figure 4i). We observed that the annealing of the conductive tracks continues when the dielectric is thermally cured; whereas the sheet resistances of the tracks still continued to decrease. Additionally, the cracking of the tracks starts to affect the measured resistances in a few samples. After the printing and curing of the topmost silver tracks, the resistance increment of the bottommost tracks is more significant due to the crack propagation.

Despite the structural degradation, over 80% of the tracks were still conductive after curing the topmost silver tracks, and

https://dx.doi.org/10.1021/acsami.9b19632
ACS Appl. Mater. Interfaces 2020, 12, 11990−11997

the mean sheet resistance was only 8% higher than the initial value. Out of the 96 measured track intersections, only five short circuits were detected in total. This result confirms the effective electrical insulation ability of the dielectric PDMS ink layer.

The resistances of the topmost silver tracks (Layer 2) tend to be slightly higher, which is most likely due to the thinning of the topmost track in the intersections. As shown in the cross-sectional scanning electron microscopy (SEM) images, the thickness of the topmost track was only 100−400 nm at the intersections (Figure 4f), which not only increases the resistance but also makes it vulnerable to the mechanical stresses. Nevertheless, most measured sheet resistance values were still under 0.3 Ω/□.

Further studies of metal cracking mechanisms would be beneficial because track cracking was observed after the repeated curing steps, even though it was decreased significantly through optimization of both the plasma parameters and ink curing conditions. When the metal NP-based systems are heated, the conductive particles form a dense, sintered structure, enabling very high conductivity at relatively low temperatures, in comparison to a bulk metal. The disadvantage of the sintered nanoscale features is that they are more vulnerable to the thermal and mechanical stresses in comparison to, for example, flake inks, where the particle size is on a macroscale.[55] To improve the stability of our ink-jetted system under stresses, the substrate could be stretched in advance to the printing steps[56] or the pattern geometry could be adjusted.[42,57] A primer layer between the elastomeric substrate and the conductive tracks could enable the deposition of crack-free metal films on PDMS, as shown recently by Ryspayeva et al.[58]

When aiming for stretchable electronics used in, for example, e-skin applications, the conductive interconnects should also be stretchable. Even though the metal tracks in our work are not stretchable as such, several, directly applicable strategies for improved conductor elongation have been presented before. In the work of Xiang et al.,[59] it was shown that the optimization of the adhesion strength of the metal film to the PDMS can improve the stretchability of the devices up to 30%. Additionally, it has been reported in the literature that by simply changing the pattern geometry from a straight line to a horse shoe-like meander line, the stretchability of the inkjet-printed nanoparticle features will increase further by 10%.[60] Recently, Abu-Khalaf et al.[42] showed that inkjet-printed meander lines on PDMS are able to withstand 19% strain, even when a radial stretching load is used. To improve the stretching of the interconnects even further, inkjet printable silver nanowires could be used instead of spherical nanoparticles.[52] Inkjet printing of silver nanowires has been shown to be possible with the Dimatix printers.[61]

Because all of these strategies demonstrate either pattern geometries or materials for inkjet-printed electronics, they are directly applicable to our approach, highlighting the applicability of the proposed multilayered fabrication process. Other compatible functional materials include, but are not limited to, inkjettable graphene, poly(3,4-ethylenedioxythiophene):poly(styrenesulfonate), and polyvinylidene fluoride−trifluoroethylene.[62,63] These materials can be used to replace metallic conductors or to add sensing functions. Printed PDMS itself has shown interesting performance as a dielectric in, for example, actuators and pressure sensors.[20,21] Therefore, the proposed multilayer process holds a great promise to the future printed electronics applications.

CONCLUSIONS

Herein, an approach for all-inkjet-printed PDMS−based electrical multilayered structures was proposed. Optimization of the solvent type and concentration was shown to have a significant effect on the PDMS printability and the shelf-life of the ink. Herein, the ink cartridge remained functional for at least 2 days, even though the silicone elastomer was mixed in advance with the cartridge filling.

The outcome was an inkjet-printable PDMS solution, which is compatible with the widely used commercial printers. Thus, a single material printer can be used to print all the functional material layers of a soft multilayered electrical system, including both the elastomeric dielectric and other functional material layers, here, the highly conductive Ag NP tracks.

We have shown that not only the fabrication of elastomer-based devices by printing is possible, but also it outstandingly simplifies the fabrication process of multilayered devices, in contrast to the conventional lithography and mold-casting processes used for PDMS patterning, which often require additional equipment, such as punching tools or stencils. Furthermore, the digital nature of inkjet printing enables the fabrication of elastic interconnects simply by modifying the patterning geometries. Therefore, this approach has great potential for any biocompatible or skin-conformable application, where selective additive patterning of silicones is desirable.

EXPERIMENTAL METHODS

Silicone Ink Preparation. Sylgard 184 (Dow Corning) was used here both as the substrate and the dielectric material. The PDMS base and the curing agent were mixed in a 10:1 ratio (base to catalyst) in all experiments. The ink solvents were IBA (98%) and octyl acetate (OA, ≥99%) (Sigma-Aldrich). The PDMS was diluted in the solvents at various weight ratios, and the solutions were stirred for 15 min at 1500 rpm before injecting them into the ink cartridges.

Silicone Ink Characterization. The viscosities of the ink components were studied using a rotational rheometer (MCR301, Anton Paar). A concentric cylinder geometry, which is suitable for low-viscosity fluids, was chosen for the measurements. The viscosity of the ink components as a function of shear rate was measured at a constant temperature of 25 °C by increasing the shear rate in logarithmic steps (6 steps/decade) from 1 to 1000 1/s. The effect of the temperature on the viscosity was studied by temperature sweep measurements, where the shear rate was a constant 10 1/s, and the temperature was increased linearly from 25 to 70 °C at a rate of 1 °C/min.

The surface tensions of the ink components were measured by the pendant drop method (Drop Shape Analyzer DSA100, Krüss GmbH). First, ultrapure water was used as a reference substance for all measurements. Surface tensions were measured using the software's Young−Laplace equation for the extracted droplet profile. Measurements were repeated for all the prepared inks.

The composition of the printed and cured elastomer inks was determined using a confocal Raman microscope (532 nm, inVia Qontor, Renishaw). An optical interferometer (Wyko NT1100, Veeco) was used to measure the thickness of the printed silicone ink, when printed on the spin-coated PDMS substrate (Sylgard 184). A thin carbon coating was sputtered onto the surface (JEOL-530, JEOL) to improve the imaging of the otherwise transparent samples.

Device Fabrication. Glass slides were cleaned by ultrasonication in a deionized water bath for 15 min, followed by an acetone bath for 15 min at 50 °C. Then, the samples were placed in a 2-propanol bath for 10 min. Finally, the slides were rinsed with deionized water, dried

https://dx.doi.org/10.1021/acsami.9b19632
ACS Appl. Mater. Interfaces 2020, 12, 11990−11997

with compressed air, and exposed to UV light for 15 min. We then spin-coated the samples (2000 rpm, 60 s) with a 1% (by weight) polytetrafluoroethylene (PTFE) solution in Fluorinert FC-40 (Sigma-Aldrich) and cured the samples at 150 °C for 10 min. Teflon coating was used to enable peeling of the PDMS samples from the glass carrier after the fabrication process was completed.

To fabricate the PDMS substrates, we first spin-coated an approximately 20 μm-thick PDMS layer on a PTFE-coated glass slide (60 s, 1600 rpm) and cured it at 120 °C for 25 min. After that, the substrate was surface-treated with nitrogen plasma (exposure power 100 W, duration 1 min, pressure 0.6 mbar, and gas flow 700 sccm) in a plasma chamber (Diener Atto, Diener electronic GmbH).

We then inkjet-printed the first conductive pattern with an Ag NP ink (Silverjet DGP-10LT-15C, Advanced Nano Products) on the substrate directly after the surface pretreament with a commercial inkjet printer (Dimatix DMP-2800, Fujifilm). The printer platen temperature was kept at 60 °C to let the inks dry and settle before curing in the oven. This two-layer print was then annealed at 120 °C for 30 min, followed by the printing of the PDMS ink on the PDMS substrate and on top of the conductive tracks, sealing the conductors. Up to eight layers of the dielectric ink were printed directly on the underlying surfaces, without any additional surface treatments. The printer platen temperature was again kept at 60 °C to prevent excessive spreading of the wet ink. When all layers had been printed, we used a hot plate to cure the elastomer ink at 120 °C for 20 min, allowing the solvent to evaporate properly and to cross-link the PDMS.

After the dielectric printing, our device was again treated with the nitrogen plasma. To prevent the plasma exposure of the nonsealed measurement pads at both ends of the cured conductive tracks, a polyethylene terephthalate (PET) foil was used as a temporary protective mask during the surface treatment.

Then, we printed an additional set of Ag tracks on top of the PDMS layer. The topmost tracks were printed perpendicular to the first silver layer, thus making the PDMS an electrically insulating layer of the multilayered lattice structure. After that, the whole system was again cured at 120 °C for 30 min to anneal the topmost Ag NPs.

Device Characterization. An optical microscope was used to measure the line widths of the printed PDMS and the silver tracks and to detect the possible cracks. The resistances of the conductive tracks were measured using a 4-wire sensing mode of a source measure unit (Keithley 2425). The sheet resistance of each track was then calculated by dividing the total resistance by the ratio of track length (36 mm) to track width (0.5 mm). These resistance measurements were repeated after printing and curing of (1) the bottommost silver tracks, (2) the dielectric PDMS ink, and (3) the topmost silver tracks. A high-resolution scanning electron microscope with a FIB (Cross-beam 540, Zeiss) was used for the cross-sectional imaging of the devices.

■ ASSOCIATED CONTENT

Supporting Information

The Supporting Information is available free of charge at https://pubs.acs.org/doi/10.1021/acsami.9b19632.

Calculated Z-numbers for each PDMS ink (PDF)

■ AUTHOR INFORMATION

Corresponding Author

Riikka Mikkonen − *Unit of Electrical Engineering, Faculty of Information Technology and Communication Sciences, Tampere University, 33720 Tampere, Finland;* orcid.org/0000-0003-2961-6821; Email: riikka.mikkonen@tuni.fi

Authors

Paula Puistola − *Unit of Electrical Engineering, Faculty of Information Technology and Communication Sciences, Tampere University, 33720 Tampere, Finland*

Ilari Jönkkäri − *Unit of Materials Science and Environmental Engineering, Faculty of Engineering and Natural Sciences, Tampere University, 33720 Tampere, Finland*

Matti Mäntysalo − *Unit of Electrical Engineering, Faculty of Information Technology and Communication Sciences, Tampere University, 33720 Tampere, Finland*

Complete contact information is available at: https://pubs.acs.org/10.1021/acsami.9b19632

Funding

This work was funded by the Academy of Finland (grant number: 292477) and Business Finland (grant number 2947/31/2018). This work was supported (in part) by the Academy of Finland "Printed Intelligence Infrastructure" (PII-FIRI, grant no. 320019). M. Mäntysalo was supported by the Academy of Finland (grant number 288945). Riikka Mikkonen would like to thank Nokia Foundation for support.

Notes

The authors declare no competing financial interest.

■ ACKNOWLEDGMENTS

This work made use of Tampere Microscopy Center Facilities at Tampere University.

■ REFERENCES

(1) Kim, J.-H.; Kim, S.-R.; Kil, H.-J.; Kim, Y.-C.; Park, J.-W. Highly Conformable, Transparent Electrodes for Epidermal Electronics. *Nano Lett.* **2018**, *18*, 4531−4540.

(2) Backman, D. E.; LeSavage, B. L.; Shah, S. B.; Wong, J. Y. A Robust Method to Generate Mechanically Anisotropic Vascular Smooth Muscle Cell Sheets for Vascular Tissue Engineering. *Macromol. Biosci.* **2017**, *17*, 1600434.

(3) Drupitha, M. P.; Bankoti, K.; Pal, P.; Das, B.; Parameswar, R.; Dhara, S.; Nando, G. B.; Naskar, K. Morphology-Induced Physico-Mechanical and Biological Characteristics of TPU−PDMS Blend Scaffolds for Skin Tissue Engineering Applications. *J. Biomed. Mater. Res. Part B Appl. Biomater.* **2019**, *107*, 1634−1644.

(4) Shuai, X.; Zhu, P.; Zeng, W.; Hu, Y.; Liang, X.; Zhang, Y.; Sun, R.; Wong, C.-p. Highly Sensitive Flexible Pressure Sensor Based on Silver Nanowires-Embedded Polydimethylsiloxane Electrode with Microarray Structure. *ACS Appl. Mater. Interfaces* **2017**, *9*, 26314−26324.

(5) Qin, D.; Xia, Y.; Whitesides, G. M. Soft Lithography for Micro- and Nanoscale Patterning. *Nat. Protoc.* **2010**, *5*, 491.

(6) Grosberg, A.; Alford, P. W.; McCain, M. L.; Parker, K. K. Ensembles of Engineered Cardiac Tissues for Physiological and Pharmacological Study: Heart on a Chip. *Lab Chip* **2011**, *11*, 4165−4173.

(7) O'Bryan, C. S.; Bhattacharjee, T.; Hart, S.; Kabb, C. P.; Schulze, K. D.; Chilakala, I.; Sumerlin, B. S.; Sawyer, W. G.; Angelini, T. E. Self-Assembled Micro-Organogels for 3D Printing Silicone Structures. *Sci. Adv.* **2017**, *3*, No. e1602800.

(8) Hinton, T. J.; Hudson, A.; Pusch, K.; Lee, A.; Feinberg, A. W. 3D Printing PDMS Elastomer in a Hydrophilic Support Bath via Freeform Reversible Embedding. *ACS Biomater. Sci. Eng.* **2016**, *2*, 1781−1786.

(9) Holländer, J.; Hakala, R.; Suominen, J.; Moritz, N.; Yliruusi, J.; Sandler, N. 3D Printed UV Light Cured Polydimethylsiloxane Devices for Drug Delivery. *Int. J. Pharm.* **2018**, *544*, 433−442.

(10) Ozbolat, V.; Dey, M.; Ayan, B.; Povilianskas, A.; Demirel, M. C.; Ozbolat, I. T. 3D Printing of PDMS Improves Its Mechanical and Cell Adhesion Properties. *ACS Biomater. Sci. Eng.* **2018**, *4*, 682−693.

(11) Patel, D. K.; Sakhaei, A. H.; Layani, M.; Zhang, B.; Ge, Q.; Magdassi, S. Highly Stretchable and UV Curable Elastomers for Digital Light Processing Based 3D Printing. *Adv. Mater.* **2017**, *29*, 1606000.

(12) Abbel, R.; Teunissen, P.; Rubingh, E.; Lammeren, T. v.; Cauchois, R.; Everaars, M.; Valeton, J.; Geijn, S. v. d.; Groen, P. Industrial-Scale Inkjet Printed Electronics Manufacturing-{\textemdash}production up-Scaling from Concept Tools to a Roll-to-Roll Pilot Line. *Transl. Mater. Res.* **2014**, *1*, 015002.
(13) Wu, J.; Wang, R.; Yu, H.; Li, G.; Xu, K.; Tien, N. C.; Roberts, R. C.; Li, D. Inkjet-Printed Microelectrodes on PDMS as Biosensors for Functionalized Microfluidic Systems. *Lab Chip* **2015**, *15*, 690−695.
(14) Sturgess, C.; Tuck, C. J.; Ashcroft, I. A.; Wildman, R. D. 3D Reactive Inkjet Printing of Polydimethylsiloxane. *J. Mater. Chem. C* **2017**, *5*, 9733−9743.
(15) Tavakoli, M.; Malakooti, M. H.; Paisana, H.; Ohm, Y.; Green Marques, D.; Alhais Lopes, P.; Piedade, A. P.; de Almeida, A. T.; Majidi, C. EGaIn-Assisted Room-Temperature Sintering of Silver Nanoparticles for Stretchable, Inkjet-Printed, Thin-Film Electronics. *Adv. Mater.* **2018**, *30*, 1801852.
(16) Gao, M.; Li, L.; Li, W.; Zhou, H.; Song, Y. Direct Writing of Patterned, Lead-Free Nanowire Aligned Flexible Piezoelectric Device. *Adv. Sci.* **2016**, *3*, 1600120.
(17) Thuau, D.; Kallitsis, K.; Dos Santos, F. D.; Hadziioannou, G. All Inkjet-Printed Piezoelectric Electronic Devices: Energy Generators, Sensors and Actuators. *J. Mater. Chem. C* **2017**, *5*, 9963−9966.
(18) Su, M.; Li, F.; Chen, S.; Huang, Z.; Qin, M.; Li, W.; Zhang, X.; Song, Y. Nanoparticle Based Curve Arrays for Multirecognition Flexible Electronics. *Adv. Mater.* **2016**, *28*, 1369−1374.
(19) Wang, S.; Xu, J.; Wang, W.; Wang, G.-J. N.; Rastak, R.; Molina-Lopez, F.; Chung, J. W.; Niu, S.; Feig, V. R.; Lopez, J.; Lei, T.; Kwon, S.-K.; Kim, Y.; Foudeh, A. M.; Ehrlich, A.; Gasperini, A.; Yun, Y.; Murmann, B.; Tok, J. B.-H.; Bao, Z. Skin Electronics from Scalable Fabrication of an Intrinsically Stretchable Transistor Array. *Nature* **2018**, *555*, 83.
(20) McCoul, D.; Rosset, S.; Schlatter, S.; Shea, H. Inkjet 3D Printing of UV and Thermal Cure Silicone Elastomers for Dielectric Elastomer Actuators. *Smart Mater. Struct.* **2017**, *26*, 125022.
(21) Peng, Y.; Xiao, S.; Yang, J.; Lin, J.; Yuan, W.; Gu, W.; Wu, X.; Cui, Z. The Elastic Microstructures of Inkjet Printed Polydimethylsiloxane as the Patterned Dielectric Layer for Pressure Sensors. *Appl. Phys. Lett.* **2017**, *110*, 261904.
(22) Lopes, P. A.; Paisana, H.; De Almeida, A. T.; Majidi, C.; Tavakoli, M. Hydroprinted Electronics: Ultrathin Stretchable Ag−In−Ga E-Skin for Bioelectronics and Human−Machine Interaction. *ACS Appl. Mater. Interfaces* **2018**, *10*, 38760−38768.
(23) Mohammed, M. G.; Kramer, R. All-Printed Flexible and Stretchable Electronics. *Adv. Mater.* **2017**, *29*, 1604965.
(24) Kong, Y. L.; Tamargo, I. A.; Kim, H.; Johnson, B. N.; Gupta, M. K.; Koh, T.-W.; Chin, H.-A.; Steingart, D. A.; Rand, B. P.; McAlpine, M. C. 3D Printed Quantum Dot Light-Emitting Diodes. *Nano Lett.* **2014**, *14*, 7017−7023.
(25) Wang, C.; Sim, K.; Chen, J.; Kim, H.; Rao, Z.; Li, Y.; Chen, W.; Song, J.; Verduzco, R.; Yu, C. Soft Ultrathin Electronics Innervated Adaptive Fully Soft Robots. *Adv. Mater.* **2018**, *30*, 1706695.
(26) Markvicka, E. J.; Bartlett, M. D.; Huang, X.; Majidi, C. An Autonomously Electrically Self-Healing Liquid Metal−Elastomer Composite for Robust Soft-Matter Robotics and Electronics. *Nat. Mater.* **2018**, *17*, 618−624.
(27) You, I.; Kong, M.; Jeong, U. Block Copolymer Elastomers for Stretchable Electronics. *Acc. Chem. Res.* **2019**, *52*, 63−72.
(28) Mamidanna, A.; Lefky, C.; Hildreth, O. Drop-on-Demand Printed Microfluidics Device with Sensing Electrodes Using Silver and PDMS Reactive Inks. *Microfluid. Nanofluid.* **2017**, *21*, 1−9.
(29) Lee, J.; Kim, J.; Park, J.; Lee, C. Characterization of in Situ Sintering of Silver Nanoparticles on Commercial Photo Papers in Inkjet Printing. *Flexible Printed Electron.* **2018**, *3*, 025001.
(30) Su, W.; Cook, B. S.; Fang, Y.; Tentzeris, M. M. Fully Inkjet-Printed Microfluidics: A Solution to Low-Cost Rapid Three-Dimensional Microfluidics Fabrication with Numerous Electrical and Sensing Applications. *Sci. Rep.* **2016**, *6*, 35111.
(31) Angelo, P. D.; Farnood, R. R. Photoluminescent Inkjet Ink Containing ZnS:Mn Nanoparticles as Pigment. *J. Exp. Nanosci.* **2011**, *6*, 473−487.
(32) Wang, Y.; Zhu, C.; Pfattner, R.; Yan, H.; Jin, L.; Chen, S.; Molina-Lopez, F.; Lissel, F.; Liu, J.; Rabiah, N. I.; Chen, Z.; Chung, J. W.; Linder, C.; Toney, M. F.; Murmann, B.; Bao, Z. A Highly Stretchable, Transparent, and Conductive Polymer. *Sci. Adv.* **2017**, *3*, No. e1602076.
(33) Grubb, P. M.; Subbaraman, H.; Park, S.; Akinwande, D.; Chen, R. T. Inkjet Printing of High Performance Transistors with Micron Order Chemically Set Gaps. *Sci. Rep.* **2017**, *7*, 1202.
(34) Huang, Q.; Al-Milaji, K. N.; Zhao, H. Inkjet Printing of Silver Nanowires for Stretchable Heaters. *ACS Appl. Nano Mater.* **2018**, *1*, 4528−4536.
(35) Sun, J.; Jiang, J.; Bao, B.; Wang, S.; He, M.; Zhang, X.; Song, Y. Fabrication of Bendable Circuits on a Polydimethylsiloxane (PDMS) Surface by Inkjet Printing Semi-Wrapped Structures. *Materials* **2016**, *9*, 253.
(36) Woo, K.; Jang, D.; Kim, Y.; Moon, J. Relationship between Printability and Rheological Behavior of Ink-Jet Conductive Inks. *Ceram. Int.* **2013**, *39*, 7015−7021.
(37) Reis, N.; Ainsley, C.; Derby, B. Ink-Jet Delivery of Particle Suspensions by Piezoelectric Droplet Ejectors. *J. Appl. Phys.* **2005**, *97*, 094903.
(38) de Gans, B.-J.; Kazancioglu, E.; Meyer, W.; Schubert, U. S. Ink-Jet Printing Polymers and Polymer Libraries Using Micropipettes. *Macromol. Rapid Commun.* **2004**, *25*, 292−296.
(39) de Gans, B.-J.; Duineveld, P. C.; Schubert, U. S. Inkjet Printing of Polymers: State of the Art and Future Developments. *Adv. Mater.* **2004**, *16*, 203−213.
(40) Tekin, E.; Smith, P. J.; Schubert, U. S. Inkjet Printing as a Deposition and Patterning Tool for Polymers and Inorganic Particles. *Soft Matter* **2008**, *4*, 703−713.
(41) Bae, S. C.; Lee, H.; Lin, Z.; Granick, S. Chemical Imaging in a Surface Forces Apparatus: Confocal Raman Spectroscopy of Confined Poly(Dimethylsiloxane). *Langmuir* **2005**, *21*, 5685−5688.
(42) Abu-Khalaf, J.; Al-Ghussain, L.; Al-Halhouli, A. a. Fabrication of Stretchable Circuits on Polydimethylsiloxane (PDMS) Pre-Stretched Substrates by Inkjet Printing Silver Nanoparticles. *Materials* **2018**, *11*, 2377.
(43) Belsey, K. E.; Parry, A. V. S.; Rumens, C. V.; Ziai, M. A.; Yeates, S. G.; Batchelor, J. C.; Holder, S. J. Switchable Disposable Passive RFID Vapour Sensors from Inkjet Printed Electronic Components Integrated with PDMS as a Stimulus Responsive. *J. Mater. Chem. C* **2017**, *5*, 3167−3175.
(44) Ko, E.-H.; Kim, H.-J.; Lee, S.-M.; Kim, T.-W.; Kim, H.-K. Stretchable Ag Electrodes with Mechanically Tunable Optical Transmittance on Wavy-Patterned PDMS Substrates. *Sci. Rep.* **2017**, *7*, 46739.
(45) Hemmilä, S.; Cauich-Rodríguez, J. V.; Kreutzer, J.; Kallio, P. Rapid, Simple, and Cost-Effective Treatments to Achieve Long-Term Hydrophilic PDMS Surfaces. *Appl. Surf. Sci.* **2012**, *258*, 9864−9875.
(46) Li, C.-Y.; Liao, Y.-C. Adhesive Stretchable Printed Conductive Thin Film Patterns on PDMS Surface with an Atmospheric Plasma Treatment. *ACS Appl. Mater. Interfaces* **2016**, *8*, 11868−11874.
(47) Jokinen, V.; Suvanto, P.; Franssila, S. Oxygen and Nitrogen Plasma Hydrophilization and Hydrophobic Recovery of Polymers. *Biomicrofluidics* **2012**, *6*, 016501.
(48) Kim, Y.; Ren, X.; Kim, J. W.; Noh, H. Direct Inkjet Printing of Micro-Scale Silver Electrodes on Polydimethylsiloxane (PDMS) Microchip. *J. Micromech. Microeng.* **2014**, *24*, 115010.
(49) Moon, K.-S.; Dong, H.; Maric, R.; Pothukuchi, S.; Hunt, A.; Wong, C. P. Thermal Behavior of Silver Nanoparticles for Low-Temperature Interconnect Applications. *J. Electron. Mater.* **2005**, *34*, 168−175.
(50) Li, J.-H.; Jang, K.-L.; Ahn, K.; Yoon, T.; Lee, T.-I.; Kim, T.-S. Thermal Expansion Behavior of Thin Films Expanding Freely on Water Surface. *Sci. Rep.* **2019**, *9*, 7071.

https://dx.doi.org/10.1021/acsami.9b19632
ACS Appl. Mater. Interfaces 2020, 12, 11990−11997

(51) Greer, J. R.; Street, R. A. Thermal Cure Effects on Electrical Performance of Nanoparticle Silver Inks. *Acta Mater.* **2007**, *55*, 6345−6349.
(52) Amjadi, M.; Pichitpajongkit, A.; Lee, S.; Ryu, S.; Park, I. Highly Stretchable and Sensitive Strain Sensor Based on Silver Nanowire−Elastomer Nanocomposite. *ACS Nano* **2014**, *8*, 5154−5163.
(53) Huang, G.-W.; Xiao, H.-M.; Fu, S.-Y. Wearable Electronics of Silver-Nanowire/Poly(Dimethylsiloxane) Nanocomposite for Smart Clothing. *Sci. Rep.* **2015**, *5*, 13971.
(54) Hilbich, D.; Gray, B. L.; Shannon, L. A Low-Cost, Micropattern Transfer Process for Thick-Film Metallization of PDMS. *J. Electrochem. Soc.* **2017**, *164*, B3067−B3076.
(55) Cronin, H. M.; Stoeva, Z.; Brown, M.; Shkunov, M.; Silva, S. R. P. Photonic Curing of Low-Cost Aqueous Silver Flake Inks for Printed Conductors with Increased Yield. *ACS Appl. Mater. Interfaces* **2018**, *10*, 21398−21410.
(56) Lee, J.; Chung, S.; Song, H.; Kim, S.; Hong, Y. Lateral-Crack-Free, Buckled, Inkjet-Printed Silver Electrodes on Highly Pre-Stretched Elastomeric Substrates. *J. Phys. D: Appl. Phys.* **2013**, *46*, 105305.
(57) Fan, J. A.; Yeo, W.-H.; Su, Y.; Hattori, Y.; Lee, W.; Jung, S.-Y.; Zhang, Y.; Liu, Z.; Cheng, H.; Falgout, L.; Bajema, M.; Coleman, T.; Gregoire, D.; Larsen, R. J.; Huang, Y.; Rogers, J. A. Fractal Design Concepts for Stretchable Electronics. *Nat. Commun.* **2014**, *5*, 3266.
(58) Ryspayeva, A.; Jones, T. D. A.; Esfahani, M. N.; Shuttleworth, M. P.; Harris, R. A.; Kay, R. W.; Desmulliez, M. P. Y.; Marques-Hueso, J. A Rapid Technique for the Direct Metallization of PDMS Substrates for Flexible and Stretchable Electronics Applications. *Microelectron. Eng.* **2019**, *209*, 35−40.
(59) Xiang, Y.; Li, T.; Suo, Z.; Vlassak, J. J. High Ductility of a Metal Film Adherent on a Polymer Substrate. *Appl. Phys. Lett.* **2005**, *87*, 161910.
(60) Jablonski, M.; Lucchini, R.; Bossuyt, F.; Vervust, T.; Vanfleteren, J.; De Vries, J. W. C.; Vena, P.; Gonzalez, M. Impact of Geometry on Stretchable Meandered Interconnect Uniaxial Tensile Extension Fatigue Reliability. *Microelectron. Reliab.* **2015**, *55*, 143−154.
(61) Finn, D. J.; Lotya, M.; Coleman, J. N. Inkjet Printing of Silver Nanowire Networks. *ACS Appl. Mater. Interfaces* **2015**, *7*, 9254−9261.
(62) Vuorinen, T.; Niittynen, J.; Kankkunen, T.; Kraft, T. M.; Mäntysalo, M. Inkjet-Printed Graphene/PEDOT:PSS Temperature Sensors on a Skin-Conformable Polyurethane Substrate. *Sci. Rep.* **2016**, *6*, 35289.
(63) Haque, R. I.; Vié, R.; Germainy, M.; Valbin, L.; Benaben, P.; Boddaert, X. Inkjet Printing of High Molecular Weight PVDF-TrFE for Flexible Electronics. *Flexible Printed Electron.* **2015**, *1*, 015001.

https://dx.doi.org/10.1021/acsami.9b19632
ACS Appl. Mater. Interfaces 2020, 12, 11990−11997